Title	Synthesis and Tunable Optical Properties of C,N-Chelated Borate Luminophores Derived from Potassium Acyltrifluoroborates
Author(s)	Taguchi, Jumpei; Matsuura, Satsuki; Seki, Tomohiro; Ito, Hajime
Citation	Chemistry, A European journal, 26(11), 2450-2455 https://doi.org/10.1002/chem.201904983
Issue Date	2020-02-21
Doc URL	http://hdl.handle.net/2115/80472
Rights	This is the peer reviewed version of the following article: J. Taguchi, S. Matsuura, T. Seki, H. Ito, Chem. Eur. J. 2020, 26, 2450, which has been published in final form at doi.org/10.1002/chem.201904983. This article may be used for non-commercial purposes in accordance with Wiley Terms and Conditions for Use of Self-Archived Versions.
Type	article (author version)
File Information	Taguchi_ChemEurJ_Mac_Boracycle.pdf

Synthesis and Tunable Optical Properties of *C*,*N*-Chelated Borate Luminophores Derived from Potassium Acyltrifluoroborates

Jumpei Taguchi,[a] Satsuki Matsuura,[a] Tomohiro Seki,[a] and Hajime Ito*[a,b]

Abstract: A new class of borate luminophores has been synthesized via a simple two-step reaction using potassium acyltrifluoroborates (KATs) as starting materials. The hydrazones obtained from reactions between KATs and 2-hydrazinopyridines followed by a cyclization resulted in the unprecedented formation of *C*,*N*-chelated six-membered bora-heterocycles. Under consideration of the results of DFT and TD-DFT calculations, we designed and synthesized four luminophores based on such bora-heterocycles, which exhibit a tunable fluorescence range from blue to red in the solid state. Moreover, one of the luminophores exhibits mechanofluorochromism from blue to yellow/green. As a result of the aforementioned mechanochromism of one of these luminophores, white-color emission was achieved by simply mixing the four luminophores.
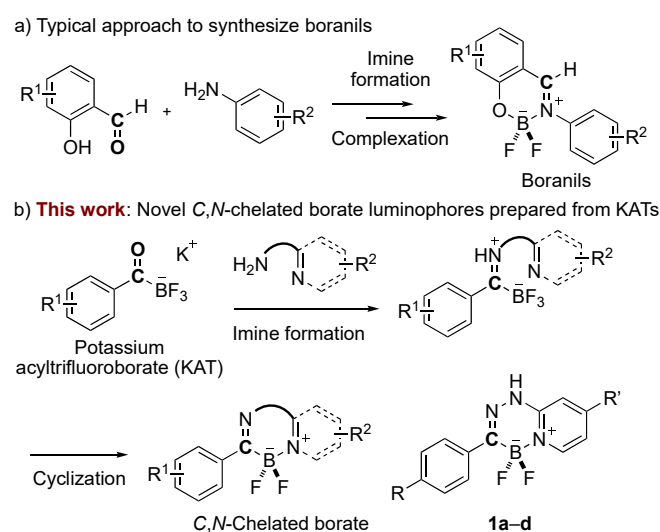
Introduction

Luminescent tetra-coordinated borates are of significant importance in organic chemistry and materials science due to their excellent optical properties and high photochemical stability.[1,2] Such compounds have already been applied in the context of fluorescence imaging, photodynamic therapy, and electroluminescence devices.[3–5] Intense efforts have also been devoted to developing a diverse range of novel borate luminophores, which includes e.g. boron-dipyrromethene (BODIPY) dyes, boron β-diketonate complexes, and boranils.[1a,1b,2]

One major factor that has driven the development of the chemistry of borate luminophores is the simplicity of their synthesis. Most of these borates are prepared by the complexation between bidentate ligands and boron electrophiles such as BF₃·Et₂O.[1] Among the reported borates, boranils are particularly attractive in terms of the facile synthesis of their *N*,*O*-chelating ligands, which can be modularly accessed by condensation reactions between substituted salicylaldehydes and anilines (Scheme 1a).[2] Furthermore, their luminescence involves an intramolecular charge transfer (ICT) state, and thus, their

emission color can be systematically tuned by employing anilines or salicylaldehydes with appropriate substituents.

Herein, we report an analogous approach to a novel class of luminescent *C*,*N*-chelated borates using potassium acyltrifluoroborates (KATs) as starting materials. Acylboron compounds exhibit a unique structure in which an inherently Lewis-acidic boryl group is directly attached to an electrophilic carbonyl carbon atom. Since the first full characterization of such a compound in 2007, the preparation and properties of acylboron derivatives have been thoroughly investigated.[6] Among various acylboron species, KATs have received particular attention due to their extraordinary stability and unique reactivity; consequently, the development of synthetic routes to KATs has reached a relatively mature stage. On the other hand, their transformation into functional compounds have received less attention and methods for their derivatization remain limited.[7] As the carbonyl group in acylborons exhibits a relatively high propensity to form imines, we attempted to apply KATs to the synthesis of bora-heterocycles via the formation of imines from a KAT and an amine that bears a coordinating *N*-heterocycle,[8] followed by a cyclization resulting in the coordination of the *N*-heterocycle to the vacant *p* orbital of the boron atom, generated by the cleavage of a B–F bond (Scheme 1b).[9] As KATs and amines with various functional groups are readily available, the resulting bora-heterocycles should exhibit a modularity that is similarly high to that of boranils. We expected that these bora-heterocycles would exhibit luminescence, given the ICT from the benzene ring of the

a) Typical approach to synthesize boranils

b) **This work**: Novel *C*,*N*-chelated borate luminophores prepared from KATs

Scheme 1. a) Representative synthesis of boranils. b) Novel *C*,*N*-chelated borate luminophores prepared from KATs (this work).

[a]   Dr. J. Taguchi, S. Matsuura, Dr. T. Seki, and Prof. Dr. H. Ito
        Division of Applied Chemistry, Graduate School of Engineering
        Hokkaido University
        Kita 13 Nishi 8 Kita-ku, Sapporo, Hokkaido 060-8628 (Japan)
        E-mail: hajito@eng.hokudai.ac.jp
[b]   Prof. Dr. H. Ito
        Institute for Chemical Reaction Design and Discovery (WPI-ICReDD), Hokkaido University
        Kita 13 Nishi 8 Kita-ku, Sapporo, Hokkaido 060-8628 (Japan)

        Supporting information for this article and crystallographic data in CIF are available on the WWW under http://dx.doi.org/xx.

KAT to the *N*-heterocycle of the amine, and thus, a judicious introduction of appropriate substituents on the benzene rings or the *N*-heterocycle could be expected to effectively tune the emission color. In addition, the dipole moment of the transition is expected to be aligned in parallel to the dipole moment, which is characteristic for stimuli-responsive luminophores.[10] This approach allowed us to access the novel *C*,*N*-chelated bora-heterocycles **1a**–**1d** from KATs and 2-hydrazinopyridines. In the solid state, **1a**–**1d** exhibit a wide range of substituent-dependent colors of luminescence. In addition, **1c** exhibits mechanofluorochromism from blue to yellow/green. Moreover, by mixing **1a**–**1d**, white-color-emitting materials can be generated due to the mechanofluorochromism of **1c**.

Results and Discussion

First, we synthesized bora-heterocycle **1a**. The reaction of 4-fluoro-substituted phenyl KAT **2a** with 2-hydrazinopyridine **3a** in the presence of acetic acid in acetonitrile smoothly furnished the corresponding hydrazone (**4a**) in 96% yield (Scheme 2).[8a] Although the condensation between KAT **2a** and 8-aminoquinoline or 2-aminopyridine was also investigated, the targeted trifluoroborate iminiums were not obtained; in the former case, **2a** decomposed, and in the latter case, only a cation exchange to ammonium occurred. Hydrazone **4a** reacts with BF₃·Et₂O in the presence of methanol to give the cyclized product (**1a**) in 91% yield.[9] To the best of our knowledge, this is the first example of the formation of a borate compound consisting of a six-membered B–N–C–N–N–C heterocycle.[11] **1a** is a pale-yellow air- and moisture-stable solid that can be isolated by column chromatography on silica gel and that exhibits blue luminescence under irradiation from UV light (*vide infra*).

In order to investigate the factors that control the emission color via variation of the substituents of **1a**, DFT and TD-DFT calculations at the B3LYP/6-31G+(d) level of theory were carried out. The results revealed two allowed transitions with large oscillator strengths (*f*), which were attributed to the transition from the highest occupied molecular orbital (HOMO) to the second-lowest unoccupied molecular orbital (LUMO+1; 319 nm; *f* = 0.5627), and to that from the HOMO to the LUMO (372 nm; *f* =
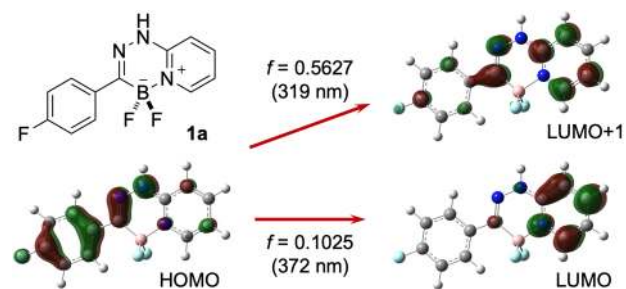

Figure 1. Calculated molecular orbitals of **1a** (B3LYP/6-31+G(d); isovalue = 0.05).

0.1025). The distribution of the calculated HOMO, LUMO, and LUMO+1 for **1a** under vacuum are shown in Figure 1. The HOMO is mostly located at the KAT-derived benzene ring, while the LUMO and the LUMO+1 are located on the pyridine ring. These results indicate that the emission can be attributed to a typical ICT. Accordingly, the emission color can be expected to be efficiently red-shifted by introduction of electron-donating groups at the benzene ring and/or electron-withdrawing groups at the pyridine ring.

Based on these calculations, we then tried to synthesize bora-heterocycles **1b**–**1d**, which contain a diphenyl amino group at the benzene ring and/or a cyano group at the pyridine ring. Cyano-substituted bora-heterocycle **1b** can be synthesized in high yield from **2a** and the corresponding hydrazine **3b** in a manner similar to that outlined before (Scheme 2; 75% over two steps). In order to synthesize amino-substituted bora-heterocycles **1c** and **1d**, the synthesis of 4-diphenyl amino-substituted phenyl KAT was investigated. A Cu(I)-catalyzed borylation of the corresponding aldehyde or a nucleophilic aromatic substitution from **2a** or **1a** were unsuccessful.[6e,12] Instead, a benzoyl trifluoroborate bearing a 4-diphenyl amino group (**2c**) was obtained from the Pd-catalyzed amination of 4-Br-substituted phenyl KAT **2b**, even though the counter cation was exchanged from potassium to tetrabutylammonium (TBA) due to the addition of an equimolar amount of TBACl given the low solubility of **2b** in toluene (Scheme 3).[13] Throughout this reaction, the acyltrifluoroborate moiety remained intact, which is consistent with the results of a previous
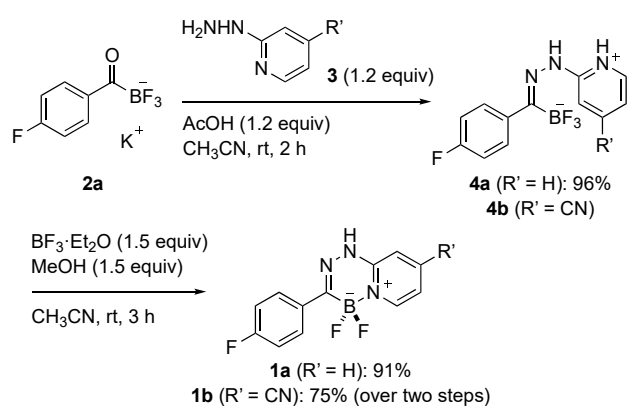
Scheme 2. Synthesis of *C*,*N*-chelated bora-heterocycles **1a** and **1b**.
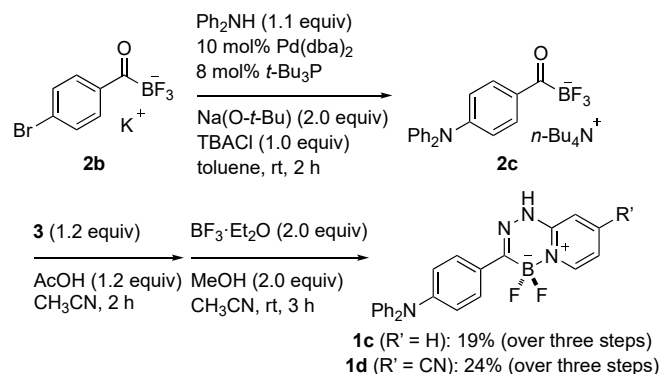
Scheme 3. Pd-catalyzed amination of 4-Br-substituted phenyl KAT **2b** and its derivatization into *C*,*N*-chelated bora-heterocycles **1c** and **1d**.
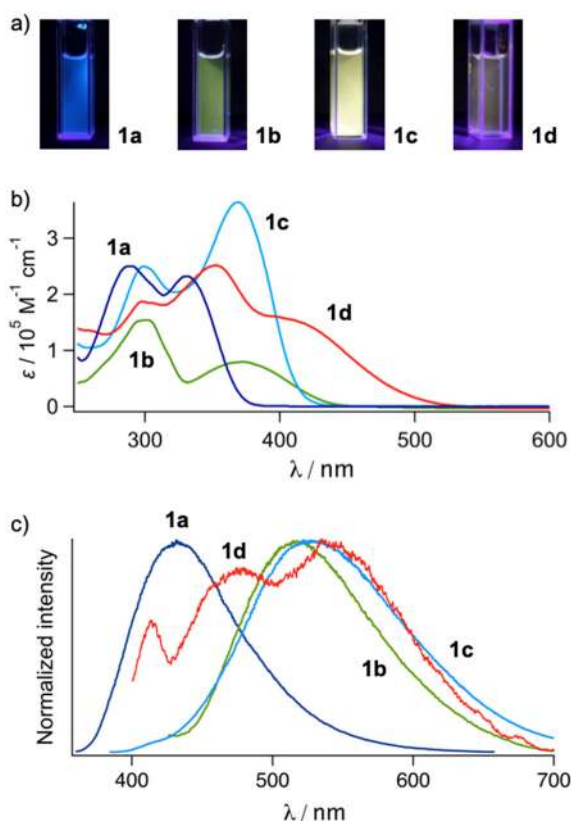
Figure 2. a) Photographs of **1a**–**1d** in acetonitrile showing different photoluminescence under illumination from UV light (λ_{ex} = 365 nm). b) Non-normalized absorption spectra of **1a**–**1d** (c = 10 µM) in acetonitrile. c) Normalized emission spectra of **1a**–**1d** (λ_{ex} = 365 nm; 10 µM) in acetonitrile.

Figure 3. a) Photographs of crystalline samples of **1a**–**1d**, which show different photoluminescence under illumination from UV light (λ_{ex} = 365 nm). b) Normalized absorption spectra of **1a**–**1d**, based on the diffuse reflection spectra. c) Normalized emission spectra of **1a**–**1d** (λ_{ex} = 365 nm).

report.[14] Using **2c** and hydrazines **3a** or **3b**, bora-heterocycles **1c** and **1d** were synthesized in moderate yield (**1c**: 19%; **1d**: 24%; over three steps from **2b**) in a manner similar to that described above.

Subsequently, we investigated the optical properties of monomeric **1a**–**1d** in acetonitrile. The solution of **1a** in acetonitrile is transparent and colorless, while those of **1b**–**1d** are transparent and pale yellow. The absorption spectrum of **1a** lies in the UV region with maxima at 288 and 330 nm (Figure 2b). These two absorption maxima correspond to the HOMO–LUMO+1 and HOMO–LUMO transitions, respectively. **1b** and **1c** also show two absorption bands, whereby the HOMO–LUMO bands (373 and 370 nm, respectively) are bathochromically shifted compared to that of **1a**. These shifts were attributed to the introduction of an electron-withdrawing cyano group at the LUMO (**1b**) and an electron-donating amino group at the HOMO region (**1c**). For **1d**, two similar absorption maxima were observed at 298 and 352 nm. Moreover, an additional shoulder emerged between 400 and 500 nm. **1a**–**1c** are weakly emissive in acetonitrile with emission quantum yields (Φ_{em}) of 2–8%. Emission lifetime measurements confirmed the fluorescence character of **1a**–**1c** (Figure S3 and Table S1). **1a** shows blue emission and a featureless emission band with a maximum at 432 nm (Figure 2c). **1b** and **1c** show similar emission bands with maxima at 517 and 522 nm,
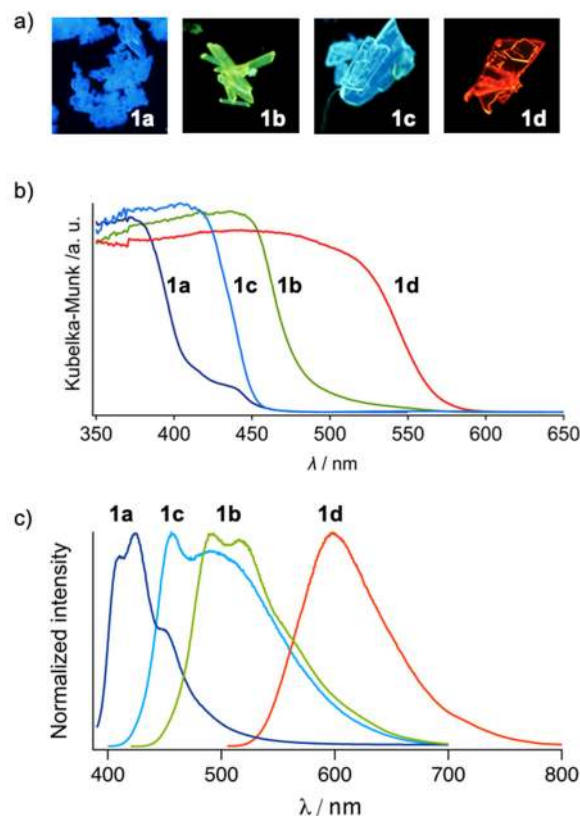
respectively, commensurate with green emission (Figure 2a). In contrast, the solution of **1d** is virtually non-emissive (Φ_{em} = 0.5 %).

The optical properties of bora-heterocycles **1a**–**1d** in the solid state are different from those in solution. In the solid bulk phase, **1a** exhibits a structured emission band that peaks at 424 nm with shoulders at 410 and 446 nm (Figure 3c). The absorption spectrum of **1a** shows a featureless band with an onset at 450 nm and a maximum at 370 nm (Figure 3b). Modifying the substituents leads to a drastic bathochromic shift of the absorption maxima from **1a** to **1c** (403 nm), **1b** (436 nm), and **1d** (450 nm), and a similar trend was observed for the onset wavelengths. This is corroborated by the results of the aforementioned TD-DFT calculations on the monomers. The excitation spectra of **1a**–**1d** exhibit the same trend (Figure S5), and the photoluminescence colors also differ depending on substituents: the emission of solid **1c** is pale blue, while that of solid **1b** is green and that of solid **1d** is red (Figure 3a). The emission maxima shift from **1a** to **1c** (456 nm), **1b** (492 nm), and **1d** (607 nm) as shown in Figure 3c. The emission maximum of **1c** is somewhat hypsochromically shifted relative to that of the acetonitrile solution, which stands in contrast to those of **1a** and **1b**, as these show similar emission spectra in the solid state and in acetonitrile. **1a**–**1d** exhibit low to moderate fluorescence quantum yields (Φ_{em} = 3–10%) and their fluorescence character was confirmed by lifetime measurements
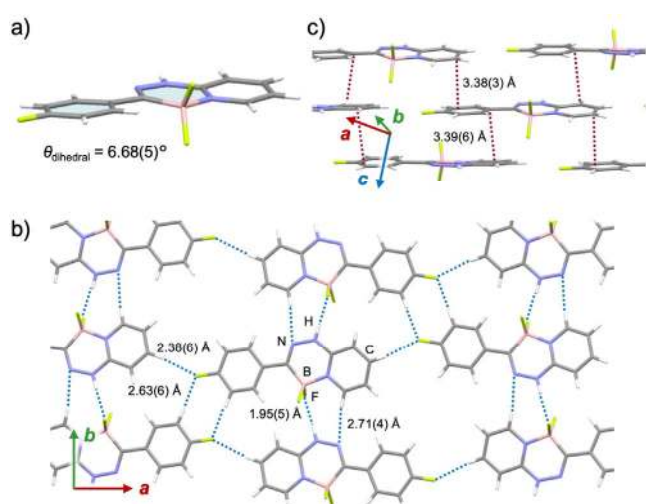
Figure 4. a) Single-crystal structure of **1a**. b) Layer structure of molecules of **1a** that arrange perpendicular to the *c* axis. c) Interactions between the layers. The crystallographic axes *a*, *b*, and *c* are depicted by arrows.

in the solid state (Figure S6 and Table S2). The emissive nature of **1a**–**1d** is different from that of typical BODIPY analogues, which are usually not emissive in the solid state.[1a]

We successfully grew single crystals of **1a**–**1d** and found that they exhibit similar packing structures (Table S4). **1a** crystallizes in the monoclinic space group $P2_1/n$, and the six-membered bora-heterocycle exhibits high planarity with a dihedral angle of 6.68(5)° between the benzene ring and the bora-heterocycle (Figure 4a). These flat molecules form multiple N–H···F–B, C–H···N, and C–H···F–C hydrogen bonds between neighboring molecules to construct 2-D molecular sheets in the *ab* plane (blue dotted line in Figure 4b). Between the molecular sheets, molecules of **1a** form π···π stacking interactions via the benzene and the pyridine rings with longitudinal displacement (Figure 4c). Such head-to-tail stacking motifs are typical for planar dipolar molecules.[15] The crystal structures of **1b**–**1d** also reveal planar conformations with dihedral angles of 0.2–11.4°. Due to these flat conformations, **1b**–**1d** also exhibit partially overlapping stacking arrangements (Figures S9b, S10b, and S11b). Perpendicular to the stacking direction, hydrogen bonds (N–H···F–B) manifest, which results in the formation of sheet-like motifs (Figures S9c, S10c, and S11c) similar to the case of **1a** (Figure 4b). In addition, **1c** and **1d** exhibit C–H···π interactions between the diphenyl amino groups, which supports the construction of the sheet motifs. Thus, regarding the flat conformation of the molecules, the stacking motifs, and the molecular sheet formation, the packing arrangements of **1a**–**1d** are comparable.

Interestingly, only **1c** shows mechanofluorochromism.[16] By applying mechanical stimuli to semi- or single-crystalline samples of blue-emitting **1c**, the emission color of the resulting powder (**1c**ground) changed to yellow/green (Figure 5a), confirming the mechanofluorochromic properties. Emission spectroscopy measurements revealed a red-shifted emission band (Figure 5b), i.e., **1c**ground shows a featureless broad emission spectrum with a
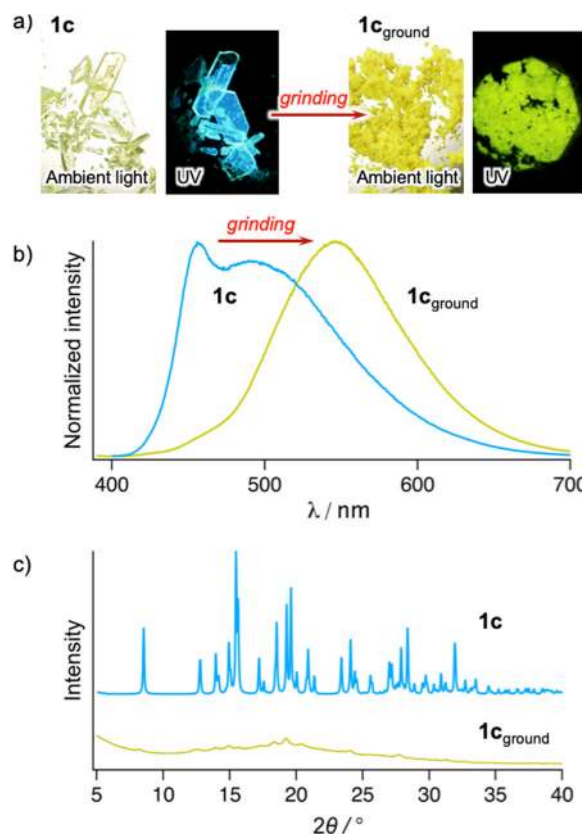

Figure 5. a) Photographs of the crystalline and ground powder samples of **1c** under ambient light and UV light (λ_{ex} = 365 nm). b) Normalized emission spectra (λ_{ex} = 365 nm) of **1c** and **1c**ground. c) Simulated PXRD pattern obtained from of the single crystal structure of **1c** (blue) and PXRD pattern of **1c**ground (yellow/green).

peak at 547 nm, which is similar to the emission spectrum of the acetonitrile solution of **1c**. In other words, the emission maximum of **1c**ground shows a bathochromic shift of 91 nm relative to that of 1c (λ_{max} = 456 nm) upon grinding. Conversely, **1a**, **1b**, and **1d** did not show mechanofluorochromism.

To gain further insight into the mechanism underlying the mechanofluorochromism of **1c**, powder X-ray diffraction analyses were conducted. After mechanical stimulation, **1c**ground exhibits a diffraction pattern with very weak intensity (yellow/green line in Figure 5c). The positions of the residual weak peaks of **1c**ground can be satisfactorily matched with those of a simulated powder pattern of **1c** derived from the single-crystal structure (blue line in Figure 5c). This result indicates that amorphization occurs upon transformation from **1c** to **1c**ground. It seems thus feasible to attribute the observed mechanochromism of **1c** to a crystal-to-amorphous phase change. Regarding the similarity of the emission spectra of **1c** in acetonitrile and **1c**ground, it seems also feasible to conclude that the emission of **1c** in the amorphous phase has a monomer character.[17]

Given that we obtained a series of luminophores that exhibit a range of fluorescence colors, we were interested to find out if we could generate white emission.[18] Indeed, simply by mixing solid samples of **1a**–**1d** (5 mg each) and grinding the thus
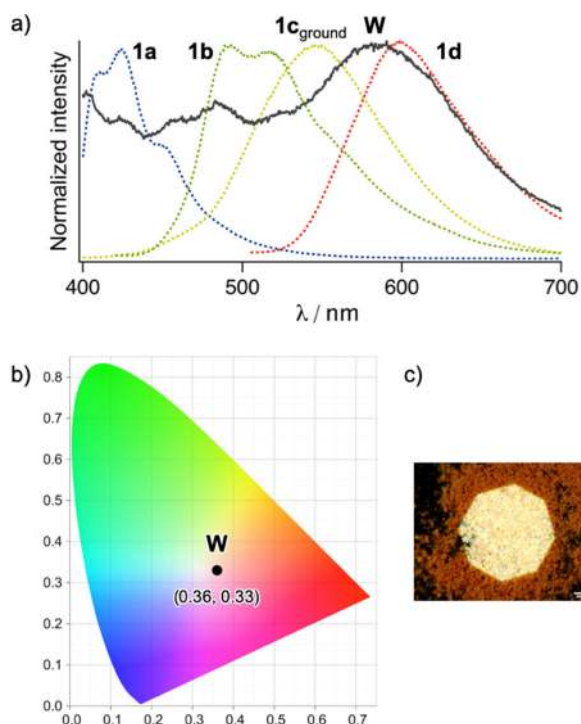
Figure 6. White emission of a mixture of **1a**–**1d** after grinding. a) Emission spectra of **1a**, **1b**, **1c**$_{ground}$, **1d**, and **W** in the solid state. b) Emission color coordinates of **W** in the CIE 1931 chromaticity diagram. C) Photograph of a powdered sample of **W** showing white emission.

obtained mixture in a ball mill for 30 min, we obtained a pale-yellow powder (**W**). Remarkably, **W** showed white emission upon photoexcitation (Figure 6c). The emission spectrum of **W** covers the entire visible region (black line in Figure 6a). After grinding, **W** should consist of **1a**, **1b**, **1c**$_{ground}$, and **1d**, considering the mechanochromic properties of **1c**. However, the emission spectrum of **W** is not simply the sum of those of **1a**, **1b**, **1c**$_{ground}$, and **1d**. This is indicative of the formation of heterogeneous molecular interactions of **1**, which are facilitated by the common molecular scaffold and the somewhat similar packing patterns. Due to the coverage of the entire visible region, the Commission Internationale de l'Éclairage (CIE) 1931 chromaticity coordinates of the emission of W (0.36, 0.33) are very close to those of pure white (0.33, 0.33) (Figure 6b).[19] A systematic optimization of the mixing ratios of **1a**–**1d** can thus be feasibly expected to generate solid materials with purely white emission.

Conclusions

In summary, we have synthesized a novel class of bora-heterocycles (**1a**–**1d**) based on the formation of imines between KATs and 2-hydrazinopyridines, followed by a cyclization. **1a**–**1d** exhibit a range of luminescent colors from blue to red in the solid state. **1c** exhibits a red-shifted mechanofluorochromism that is based on a crystal-to-amorphous transition. Furthermore, white emission was achieved simply by mixing **1a**–**1d** and grinding. As

the unique structure of the KATs enables the first synthesis of these borate luminophores, we believe that this method allows applying KATs to luminescent materials. Further investigations into the synthesis of related classes of bora-heterocycles are currently in progress in our laboratory, and the results will be reported in due course.

[1]   (a) G. Ulrich, R. Ziessel, A. Harriman, *Angew. Chem., Int. Ed.* **2008**, *47*, 1184–1201; (b) P.-Z. Chen, L.-Y. Niu, Y.-Z. Chen, Q.-Z. Yang, *Coord. Chem. Rev.* **2017**, *350*, 196–216; (c) D. Frath, J. Massue, G. Ulrich, R. Ziessel, *Angew. Chem., Int. Ed.* **2014**, *53*, 2290–2310.

[2]   (a) D. Frath, S. Azizi, G. Ulrich, P. Retailleau, R. Ziessel, *Org. Lett.* **2011**, *13*, 3414–3417; (b) J. Dobkowski, P. Wnuk, J. Buczyńska, M. Pszona, G. Orzanowska, D. Frath, G. Ulrich, J. Massue, S. Mosquera-Vázquez, E. Vauthey, C. Radzewicz, R. Ziessel, J. Waluk, *Chem.-Eur. J.* **2015**, *21*, 1312–1327; (c) G. Wesela-Bauman, M. Urban, S. Luliński, J. Serwatowski, K. Woźniak, *Org. Biomol. Chem.* **2015**, *13*, 3268–3279; (d) D. Frath, K. Benelhadj, M. Munch, J. Massue, G. Ulrich, *J. Org. Chem.* **2016**, *81*, 9658–9668; (e) D. Frath, P. Didier, Y. Mély, J. Massue, G. Ulrich, ChemPhotoChem **2017**, *1*, 109–112; (f) M. Urban, K. Durka, P. Jankowski, J. Serwatowski, S. Luliński, *J. Org. Chem.* **2017**, *82*, 8234–8241; (g) P. Zhang, W. Liu, G. Niu, H. Xiao, M. Wang, J. Ge, J. Wu, H. Zhang, Y. Li, P. Wang, *J. Org. Chem.* **2017**, *82*, 3456–3462; (h) S. Shah, A. Bajaj, A. Shibu, Md. E. Ali, P. P. Neelakandan, *Chem. Eur. J.* **2018**, *24*, 18788–18794.

[3]   T. Kowada, H. Maeda, K. Kikuchi, *Chem. Soc. Rev.* **2015**, *44*, 4953–4972.

[4]   A. Turksoy, D. Yildiz, E. U. Akkaya, *Coord. Chem. Rev.* **2019**, *379*, 47–64.

[5]   (a) Y. L. Rao, S. Wang, *Inorg. Chem.* **2011**, *50*, 12263–12274; (b) D. Li, H. Zhang, Y. Wang, *Chem. Soc. Rev.* **2013**, *42*, 8416–8433.

[6]   (a) F. K. Scharnagl, S. K. Bose, T. B. Marder, *Org. Biomol. Chem.* **2017**, *15*, 1738–1752; (b) S. M. Liu, D. Wu, J. W. Bode, *Org. Lett.* **2018**, *20*, 2378–2381; (c) J. Taguchi, T. Ikeda, R. Takahashi, I. Sasaki, Y. Ogasawara, T. Dairi, N. Kato, Y. Yamamoto, J. W. Bode, H. Ito, *Angew. Chem., Int. Ed.* **2017**, *56*, 13847–13851; (d) M. L. Lepage, S. Lai, N. Peressin, R. Hadjerci, B. O. Patrick, D. M. Perrin, *Angew. Chem., Int. Ed.* **2017**, *56*, 15257–15261; (e) J. Taguchi, T. Takeuchi, R. Takahashi, F. Masero, H. Ito, *Angew. Chem., Int. Ed.* **2019**, *58*, 7299–7303; (f) S. Lin, L. Wang, N. Aminoleslami, Y. Lao, C. Yagel, A. Sharma, *Chem. Sci.* **2019**, *10*, 4684–4691; (g) D. Wu, N. A. Fohn, J. W. Bode, *Angew. Chem., Int. Ed.* **2019**, *58*, 11058–11062.

[7]   (a) S. Adachi, S. K. Liew, C. F. Lee, A. Lough, Z. He, J. D. S. Denis, G. Poda, A. K. Yudin, *Org. Lett.* **2015**, *17*, 5594–5597; (b) C. F. Lee, A. Holownia, J. M. Bennett, J. M. Elkins, J. D. St. Denis, S. Adachi, A. K. Yudin, *Angew. Chem., Int. Ed.* **2017**, *56*, 6264–6267; (c) D. Mazunin, N. Broguiere, M. Zenobi-Wong, J. W. Bode, *ACS Biomater. Sci. Eng.* **2015**, *1*, 456–462; (d) D. Mazunin, J. W. Bode, *Helv. Chim. Acta* **2017**, *100*,

e1600311; (e) D. Schauenburg, A. O. Gálveza, J. W. Bode, *J. Mater. Chem. B* **2018**, *6*, 4775–4782.

[8] (a) T. Shiro, A. Schuhmacher, M. K. Jackl, J. W. Bode, *Chem. Sci.* **2018**, *9*, 5191–5196; (b) D. B. Diaz, C. C. G. Scully, S. K. Liew, S. Adachi, P. Trinchera, J. D. St Denis, A. K. Yudin, *Angew. Chem., Int. Ed.* **2016**, *55*, 12659–12663.

[9] (a) H. Noda, J. W. Bode, *Org. Biomol. Chem.* **2015**, *14*, 16–20; (b) H. Noda, J. W. Bode, *Chem. Sci.*, **2014**, *5*, 4328–4332.

[10] T. Seki, Y. Takamatsu, H. Ito, *J. Am. Chem. Soc.* **2016**, 138, 6252–6260.

[11] A similar bora-heterocycle has previously been obtained from the reaction between an NHC and 9-BBN, although the boron atom adopts a trigonal-planner coordination mode in this compound. For details, see: J. J. Clarke, P. Eisenberger, S. S. Piotrkowski, C. M. Crudden, *Dalton Trans.* **2018**, *47*, 1791–1795.

[12] H. Noda, G. Erós, J. W. Bode, *J. Am. Chem. Soc.* **2014**, *136*, 5611–5614.

[13] J. F. Hartwig, M. Kawatsura, S. I. Hauck, K. H. Shaughnessy, L. M. Alcazar-Roman, *J. Org. Chem.* **1999**, *64*, 5575–5580.

[14] G. A. Molander, J. Raushel, N. M. Ellis, *J. Org. Chem.* **2010**, *75*, 4304–4306.

[15] J. Wu, Y. Cheng, J. Lan, D. Wu, S. Qian, L. Yan, Z. He, X. Li, K. Wang, B. Zou, J. You, *J. Am. Chem. Soc.* **2016**, *138*, 12803–12812.

[16] (a) S. K. Mellerup, S. Wang, *Chem. Soc. Rev.* **2019**, *48*, 3537–3549; (b) Y. Sagara; S. Yamane; M. Mitani; C. Weder; T. Kato, *Adv. Mater.* **2016**, *28*, 1073–1095; (c) M. Louis, A. Brosseau, R. Guillot, F. Ito, C. Allain, R. Métivier, *J. Phys. Chem. C* **2017**, *121*,15897–15907; (d) L. Wilbraham, M. Louis, D. Alberga, A. Brosseau, R. Guillot, F. Ito, F. Labat, R. Metivier, C. Allain, I. Ciofini, *Adv. Mater.* **2018**, *30*, 1800817; (e) M. Louis, R. Sethy, J. Kumar, S. Katao, R. Guillot, T. Nakashima, C. Allain, T. Kawai, R. Métivier, *Chem. Sci.* **2019**, *10*, 843–847; (f) J. Zhao, Z. Chi, Y. Zhang, Z. Mao, Z. Yang, E. Ubba, Z. Chi, *J. Mater. Chem. C* **2018**, *6*, 6327–6353.

[17] (a) Y. Sagara, T. Kato, *Nat. Chem.* **2009**, *1*, 605–610; (b) S.-J. Yoon, J. W. Chung, J. Gierschner, K. S. Kim, M.-G. Choi, D. Kim, S. Y. Park, *J. Am. Chem. Soc.* **2010**, *132*, 13675–13683; (c) T. Seki, K. Kashiyama, H. Ito, *Dalton Trans.* **2019**, *48*, 7105–7109.

[18] (a) S. Mukherjee, P. Thilagar, *Dyes Pigm.* **2014**, *110*, 2–27; (b) T. Seki, S. Kurenuma, H. Ito, *Chem.-Eur. J.* **2013**, *19*, 16214–16220; (c) S. K. Sarkar, G. R. Kumar, P. Thilagar, *Chem. Commun.* **2016**, *52*, 4175–4178.

[19] Ohta, N.; Robertson, A. In Colorimetry: Fundamentals and Applications; Kriss, M. A., Ed.; The Wiley-IS&T Series in Imaging Science and Technology; John Wiley & Sons Ltd.: New York, **2005**.

Entry for the Table of Contents

FULL PAPER
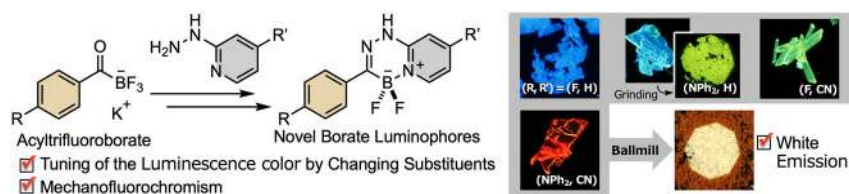
A new class of borate luminophores has been synthesized from acyltrifluoroborates as starting materials. They exhibited a wide range of luminescence colors from blue to red. One of the luminophores exhibited mechanofluorochromism from blue to yellow/green. White emission could thus be achieved simply by mixing the four obtained luminophores.

Jumpei Taguchi, Satsuki Matsuura, Tomohiro Seki, Hajime Ito*

Page No. – Page No.

Synthesis and Tunable Optical Properties of *C,N*-Chelated Borate Luminophores Derived from Potassium Acyltrifluoroborates